Interplay of Coulomb, exchange, and spin-orbit effects in semiconductor nanocrystallites

M. Chamarro, M. Dib, and V. Voliotis
Groupe de Physique des Solides, CNRS, Université Paris 6 et 7, 2 Place Jussieu, 75251 Paris Cedex 05, France

A. Filoramo and P. Roussignol
Laboratoire de Physique de la Matière Condensée, Ecole Normale Supérieure, 24 Rue Lhomond, 75005 Paris, France

T. Gacoin and J. P. Boilot
Laboratoire de Physique de la Matière Condensée, CNRS, Ecole Polytechnique, 91128 Palaiseau Cedex, France

C. Delerue, G. Allan, and M. Lannoo
Institut d'Electronique et de Microélectronique du Nord, 41 Boulevard Vauban, 59046 Lille Cedex, France
(Received 4 August 1997)

Size-selective spectroscopic techniques and a tight-binding calculation with restricted configuration interaction have been used to study the relative effects of Coulomb, exchange, and spin-orbit coupling terms on the size dependence of the lowest optical transitions in CdS nanocrystallites. Quantitative agreement is obtained for the magnitude of the corresponding dominant transitions. The nature of the states is analyzed on the basis of a simple model. A brief comparison to other semiconductor nanocrystallites like CdSe is finally presented. [S0163-1829(98)02604-6]

Semiconductor nanocrystals (SNC's) provide a major opportunity for checking current theories of electron-hole interaction in confined systems. Indeed their electronic structure is determined by the relative importance of different terms: the confinement induced level splitting, the electron-hole Coulomb and exchange interactions, and the spin-orbit coupling. The first three terms increase substantially but in a different way when the size of the SNC's is decreased into the nm range. This means that size selection and control offer a powerful way of varying the relative values of the different parameters in such a way that comparison between experiment and theory becomes a stringent test of the accuracy of the latter. Of course the size dependence of such parameters is not a new phenomenon. For instance, it was shown recently, using high-resolution spectroscopic techniques, that the exchange splitting is strongly enhanced for small SNC's. Indeed the increasing redshift with respect to the laser light observed in resonant luminescent spectra of Si,[1] CdSe,[2,3] and InP (Ref. 4) has been interpreted on this basis. From the theoretical point of view a detailed application of the effective-mass approximation (EMA) has been worked out for CdSe for which the situation is strongly simplified by the fact that the spin-orbit coupling is large compared to the other interactions.[5] The agreement with experiment was found to be qualitatively good. However, some discrepancies were observed for SNC's having a radius of the order of the bulk exciton Bohr radius.[5] Several authors[3,6] have noticed that the calculated exchange splitting underestimates the observed redshift for small SNC's. This is not too surprising since the validity of EMA in that limit is questionable.[7,8]

The aim of this paper is to perform a detailed comparison between experiment and theory in the physically interesting situation where there is a crossover in the values of the parameters. We have chosen the case of CdS SNC's, which are ideally suited to such a study, with a smaller spin-orbit coupling[9] and dielectric constant.[10,11] From the experimental point of view we use size-selective spectroscopic techniques, resonant photoluminescence (RPL) and photoluminescence excitation (PLE). Both are based on the use of a narrow energy window, either in excitation or in detection of the luminescence, which automatically selects SNC's with levels in the corresponding energy range. Theoretically we perform a nonperturbative calculation of the excitonic states, based on a tight-binding expansion of the one-particle states. In both cases we plot the level splittings vs the corresponding luminescence energies. This procedure allows a much better comparison than a plot of these quantities vs size, which is much more delicate to determine accurately. We show that one obtains good agreement over the whole range of situations not only for the level splittings but also for the oscillator strength of the transitions. We also provide a simple analytical description of overall behavior and the nature of the dominant states.

Our samples contain CdS SNC's homogeneously dispersed in a mixed organic/inorganic sol-gel silica matrix. The synthesis of the material was achieved following a process previously described.[12] From high-resolution transmission electron microscopy,[13] the average diameter was found equal to 2.7 nm with a mean standard deviation of the order of 0.7 nm. The shape of these SNC's is nearly spherical and the cubic crystalline structure was observed without evident structural defects. Resonant or nonresonant excitation was provided by a frequency doubled cw mode-locked Tsunami Ti-Sa laser pumped by an Ar^+ laser with a repetition rate of 82 MHz and a 2-ps pulse duration. The spectral resolution is about 1 meV. Nonresonant PL of the studied sample shows two bands. The lower energy one is often observed in CdS

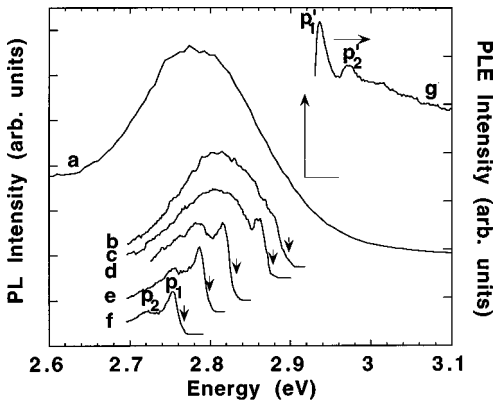

FIG. 1. PL spectra of a silica gel containing CdS NC's with 27-Å average diameter obtained at 10 K. Curve (a) shows the blue energy side of the nonresonant PL spectrum for an excitation energy of 3.444 eV. Arrows indicate the excitation energy positions for each resonant PL spectrum: curve (b) 2.898 eV, (c) 2.878 eV; (d) 2.833 eV; (e) 2.798 eV; (f) 2.766 eV. A typical PLE spectrum is represented in curve (g) detected at 2.917 eV. The arrow indicates the detection energy.

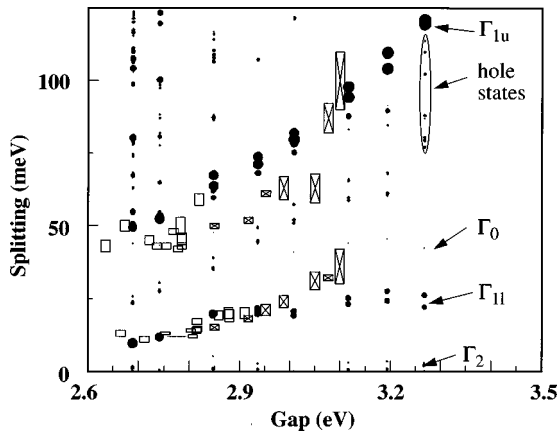

FIG. 2. Experiments: in RPL (rectangles), differences ΔE_1 and ΔE_2 between the excitation energy and the energies of the band maxima plotted as a function of the energy positions E_1 and E_2 of these two maxima; in PLE (crossed rectangles), differences $\Delta E_1'$ and $\Delta E_2'$ between the energies of these band maxima and the detection energy. The size of the rectangles gives the experimental uncertainty. Theory (dots): differences in energy between the exciton states and the lowest one versus the gap energy. The width of the dots is proportional to the oscillator strength (log scale).

colloids and is attributed to the recombination of trapped charge carriers.[14] However, the higher energy PL band is related with a more intrinsic recombination mechanism. Figure 1 shows the higher energy side of the PL spectrum obtained at 10 K for an excitation energy equal to 3.444 eV (curve a). A distribution of SNC sizes contribute to this PL. By selecting a narrow energy window in the red side of the lowest absorption band we excite only the lowest transitions of the biggest SNC's. The corresponding selectively excited RPL spectra are also shown in Fig. 1 for different excitation energies (curves $b-f$). They reveal narrower bands than the emission corresponding to the entire distribution. When the excitation energy is decreased from 2.898 eV the corresponding RPL spectrum is dominated by two bands. The differences ΔE_1 and ΔE_2 between the excitation energy and the energies of the band maxima are plotted in Fig. 2 as a function of the energy positions E_1 and E_2 of these two maxima. Furthermore, time-resolved experiments[15] show that RPL arising from these two bands exhibits a nonexponential behavior, the longest time constant being of the order of μs. Resonant PLE experiments have also been used to observe the properties of smaller SNC's. Figure 1 shows a typical PLE spectrum obtained for a detection energy equal to 2.917 eV (curve g). Again two bands are observed with, sometimes, a third one also distinguishable at a higher detection energy. The differences $\Delta E_1'$ and $\Delta E_2'$ between the energies of these band maxima and the detection energy are also represented in Fig. 2 as a function of the detection energy.

Let us now describe our calculations, which are based on a restricted configuration interaction technique.[8] As the first step, we calculate the one-electron states of the CdS SNC's using a tight-binding framework that includes interactions up to the second nearest neighbors as well as the three centers integrals. The parameters of the Hamiltonian are adjusted to get a good description of the bulk cubic CdS band structure, in particular, of the conduction band. Spin-orbit coupling is not yet included in this calculation. We then consider spherical SNC's centered at the middle of a Cd-S bond. The dangling bonds at the surface are saturated by pseudohydrogen atoms to avoid spurious localized states in the band gap. We diagonalize the corresponding matrix to get the cluster one-particle eigenstates. As the second step, the exciton wave function $|\psi_{\mathrm{exc}}\rangle$ is written as

$$|\psi_{\mathrm{exc}}\rangle=\sum_{i,j} a_{ij}|\psi_j^v\rightarrow\psi_i^c\rangle, \tag{1}$$

where $|\psi_j^v\rightarrow\psi_i^c\rangle$ is the Slater determinant corresponding to the excitation of one electron from the valence state $|\psi_j^v\rangle$ to the conduction state $|\psi_i^c\rangle$ and a_{ij} represents variational parameters. Then we write the matrix elements of the total Hamiltonian including Coulomb and spin-orbit interactions between the determinants following the rules given in Ref. 8. The intra-atomic exchange and Coulomb integrals are calculated numerically using the atomic wave functions of Ref. 16. The matrix elements of the Coulomb interaction between determinants include Coulomb and exchange integrals between one-electron states. Following the arguments of Ref. 17, and contrary to Ref. 8, the exchange integrals are left unscreened. On the other hand, the Coulomb integrals are screened using the dielectric constant given in Ref. 18, which varies with the SNC size[19] and with the distance between the two interacting particles [due to the difference between the static (ε_0) and dynamic (ε_∞) dielectric constants]. We have used $\varepsilon_0=9.12$,[10] $\varepsilon_\infty=5.27$,[11] and spin-orbit coupling constants of bulk CdS deduced from Ref. 9. The expansion in Eq. (1) is limited to a reasonable number of determinants, taken to be such that the results of two successive computations do not differ by more than 0.1 meV for the exciton binding energy. Due to the asymmetry of the valence and

conduction bands of bulk CdS we found it necessary to include the 4 lower conduction and the 24 higher valence states. The results of this calculation are plotted in Fig. 2 exactly in the same manner as done for the experimental results, i.e., they give the differences in energy ΔE between the exciton states and the lowest one versus the gap energy determined from this lowest exciton energy. On the same figure, the size of the black spots is taken proportional to the oscillator strength (on a log scale) of the transition to the ground state calculated in the same way as in Ref. 20. We can see that there is strikingly good agreement between experiment and theory, obtained with no adjustable parameters as will be discussed in the following.

To get a better understanding of these results let us show that they can be interpreted in simple terms considering an exciton formed by an electron in an s state and by a hole in x,y,z states. Including the spin of each particle ($\uparrow$ or $\downarrow$) one gets 12 composed states for the exciton, such as for example $|s_\uparrow x_\downarrow\rangle$. The exchange interaction Δ_x alone splits these states into two manifolds characterized by a total spin $S=1$ for the lowest one and by $S=0$ for the other one, their splitting being equal to Δ_x (the orbital degeneracy x,y,z remains). In this limit, only the optical transitions from the $S=0$ states to the ground state are allowed. Introducing now the spin-orbit coupling written as $-\lambda \vec{l}\cdot\vec{s}$ (the $-$ sign being due to the fact that we consider hole states) further splits the $S=1$ states into three manifolds characterized by a total momentum $J=2$, 1, and 0, respectively, denoted Γ_2, Γ_{1l}, and Γ_0; the $S=0$ states give rise to Γ_{1u} with $J=1$. The spin-orbit coupling also mixes Γ_{1l} and Γ_{1u} with the important consequence that the states Γ_{1l} become optically allowed. The calculation of the Hamiltonian matrix including exchange and spin-orbit coupling is straightforward and its eigenstates are obtained directly using momentum addition theory. The level structure is given in Fig. 3. The level splittings $\Gamma_0-\Gamma_2$, $\Gamma_{1l}-\Gamma_2$ and $\Gamma_{1u}-\Gamma_2$ are, respectively, $3\lambda/2$ and $3\lambda/4+\Delta_x/2 \pm \sqrt{(\Delta_x/6-3\lambda/4)^2+\frac{2}{9}\Delta_x^2}$. As Δ_x strongly varies with the SNC size, two asymptotic regimes emerge. For the smallest SNC's where ($\Delta_x \gg \lambda$), the $\Gamma_{1u}-\Gamma_2$ splitting varies like Δ_x while for the biggest SNC's ($\Delta_x \ll \lambda$), it saturates at $3\lambda/2$. The variations of $\Gamma_{1l}-\Gamma_2$ are much weaker with Δ_x as it always lies between 0 and $3\lambda/2$. This simple model nicely explains the results of the whole calculation (Fig. 2). The lowest exciton state is composed of five states derived from Γ_2 that are almost degenerate with a total splitting of less than 4 meV. This state is characterized by long radiative lifetimes between 1 ms and 10 μs. Between 10 and 20 meV above, there is another group of three states (Γ_{1l}) with shorter lifetimes between 10 and 0.1 μs. At $\sim$45 meV above the lowest state, a single state (Γ_0) is characterized by an almost zero transition probability. Then at upper energies there is a large group of states, two of them being strongly allowed and almost degenerate states with lifetimes of the order of 10 ns. They include the Γ_{1u} states but also states corresponding to excited states of the hole that are not included in the simple model.

We are now in position to explain the experimental results. In RPL experiments, an excitation on the red side of the absorption spectrum excites mainly SNC's with two different sizes R_1 and R_2. Resonant absorption of laser light

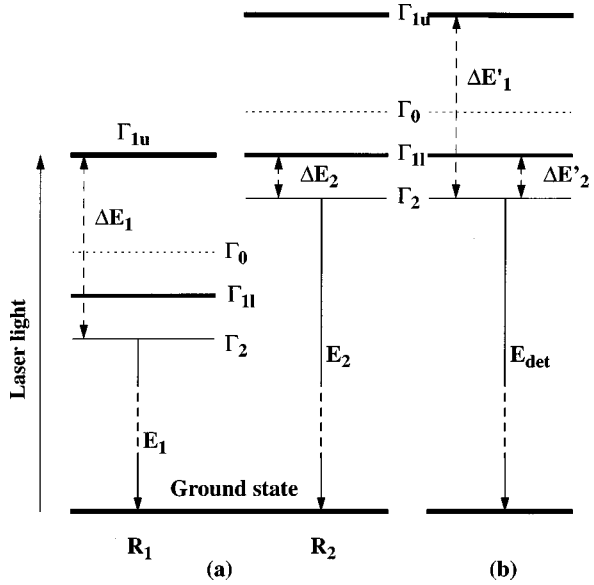

FIG. 3. Scheme of the lowest energy levels as seen by the two experiments: (a) in RPL, a laser light resonantly excites mainly SNC's with two different sizes, R_1 and R_2 ($R_1>R_2$), via Γ_{1u} and Γ_{1l}, respectively; (b) in PLE, one resonantly detects the luminescence ($E_{\rm det}$) from Γ_2, selecting essentially one cluster size, the excitation occurring via Γ_{1l} or Γ_{1u}.

creates slightly allowed excitons in Γ_{1l} for SNC's with radius R_2 but also allowed excitons in Γ_{1u} for larger SNC's of radius R_1. In both cases relaxation to the lowest exciton states Γ_2 is followed by the observation of luminescence at energies E_1 or E_2 equal to the energy of excitation minus ΔE_2 or ΔE_1, respectively. In PLE experiments, one resonantly detects the luminescence from Γ_2, selecting essentially one cluster size, the excitation occurring via Γ_{1l} or Γ_{1u} as before, giving rise to two different bands as observed. Thus, $\Delta E_1'$ and $\Delta E_2'$ correspond to the splitting $\Gamma_{1u}-\Gamma_2$ and $\Gamma_{1l}-\Gamma_2$, respectively. Note that the excitation through Γ_0 is not observed simply because of its very low oscillator strength.

In conclusion we have performed combined experimental and theoretical studies of CdS nanocrystallites with sizes in the 2-nm range. We have used size-selective resonant photoluminescence techniques and determined the different excitonic splittings vs the gap energy. We have shown that the experimental data can be fully interpreted by using a tight-binding method with restricted configuration interaction, incorporating Coulomb, exchange, and spin-orbit coupling terms. This technique is ideally suited to the treatment of such large clusters ($\sim$4000 atoms) and involves no parameter adjustable to the cluster problem (all of them are either transferred from the bulk or directly calculated). The physical nature of the lowest states has also been elucidated with a simple model. Contrary to the case of CdSe nanocrystallites,[2,3] this agreement is obtained without invoking LO phonon replica. This does not mean, however, that such replica do not exist. Indeed the LO phonon energy of bulk CdS is 36 meV, which would fall in the same energy range as the second peak (P_2 or P_2') in Fig. 2 at least for

crystallites with a gap smaller than 3.1 eV. It would even correctly predict the position of the small third peak seen, e.g., in the PLE spectrum of Fig. 1. On the other hand, phonon replica could not account for the peak positions of crystallites with a gap equal to or larger than 3.1 eV on Fig. 2.

We thank C. Guenaud and C. Delalande for helpful experimental support, in particular to obtain PLE spectra. The ''Institut d'Electronique et de Microélectronique du Nord'' is ''Unité Mixte 9929 du Centre National de la Recherche Scientifique.''

[1] P. D. J. Calcott, K. J. Nash, L. T. Canham, M. J. Kane, and D. Brumhead, J. Phys.: Condens. Matter **5**, L91 (1993).

[2] M. Chamarro, C. Gourdon, P. Lavallard, and A. I. Ekimov, Jpn. J. Appl. Phys., Part 1 **34**, Suppl. 34–1, 12 (1995); M. Chamarro, C. Gourdon, P. Lavallard, O. Lublinskaya, and A. I. Ekimov, Phys. Rev. B **53**, 1336 (1996).

[3] M. Nirmal, D. J. Norris, M. Kuno, M. G. Bawendi, Al. L. Efros, and M. Rosen, Phys. Rev. Lett. **75**, 3728 (1995).

[4] O. I. Micic, H. M. Cheong, H. Fu, A. Zunger, J. R. Sprague, A. Mascarenhas, and A. J. Nozik, J. Phys. Chem. **B101**, 4904 (1997).

[5] D. J. Norris, A. L. Efros, M. Rosen, and M. G. Bawendi, Phys. Rev. B **53**, 16 347 (1996).

[6] M. Chamarro, M. Dib, C. Gourdon, Ph. Lavallard, M. Gandais, O. Lublinskaya, and A. I. Ekimov, in *Advances in Microcrystalline and Nanocrystalline Semiconductors-1996*, edited by R. W. Collins, P. M. Fauchet, I. Shimizu, J.-C. Vial, T. Shimada, and A. P. Alivisatos, MRS Symposia Proceedings No. 452 (Materials Research Society, Pittsburgh, 1997), p. 341.

[7] A. Franceschetti and A. Zunger, Phys. Rev. Lett. **78**, 915 (1997).

[8] E. Martin, C. Delerue, G. Allan, and M. Lannoo, Phys. Rev. B **50**, 18 258 (1994).

[9] L. M. Ramaniah and S. V. Nair, Phys. Rev. B **47**, 7132 (1993).

[10] C. A. Arguello, D. L. Rousseau, and S. P. S. Porto, Phys. Rev. **181**, 1351 (1969).

[11] H. W. Verleur and A. S. Barker, Phys. Rev. **155**, 750 (1967).

[12] T. Gacoin, F. Chaput, and J. P. Boilot, J. Sol-Gel Sci. Technol. **2**, 679 (1994).

[13] T. Gacoin, C. Train, F. Chaput, J. P. Boilot, P. Aubert, M. Gandais, M. Wang, and A. Lecomte, Proc. SPIE **1758**, 565 (1992).

[14] J. J. Ramsden, S. E. Webber, and M. Gratzel, J. Phys. Chem. **89**, 2740 (1985).

[15] M. Dib (unpublished).

[16] F. Herman and S. Skillman, *Atomic Structure Calculations* (Prentice-Hall, New York, 1963).

[17] T. Takagahara and K. Takeda, Phys. Rev. B **53**, R4205 (1996).

[18] L. W. Wang and A. Zunger, Phys. Rev. B **53**, 9579 (1996).

[19] R. Tsu and D. Babic, Appl. Phys. Lett. **64**, 1806 (1994); L. W. Wang and A. Zunger, Phys. Rev. Lett. **73**, 1039 (1994); M. Lannoo, C. Delerue, and G. Allan, *ibid.* **74**, 3415 (1995).

[20] C. Delerue, G. Allan, and M. Lannoo, Phys. Rev. B **48**, 11 024 (1993).